Indole-3-carbinol-induced death in cancer cells involves EGFR downregulation and is exacerbated in a 3D environment.

Running title: Indole-3-carbinol-induced cell death

Elena P. Moiseeva, Louise H. Fox, Lynne M. Howells, Louis A. F. Temple and Margaret M. Manson.

Cancer Biomarkers and Prevention Group, Departments of Biochemistry and Cancer Studies, University of Leicester, Leicester LE1 7RH, UK.

Corresponding author: Elena P. Moiseeva

Cancer Biomarkers and Prevention Group, Departments of Biochemistry and Cancer Studies, University of Leicester, Leicester LE1 7RH, UK. em9@le.ac.uk

This work was funded by the UK Medical Research Council Grant No.G0100872.

Abstract (211 words)

Indole-3-carbinol (I3C) is a promising anticancer dietary compound, which inhibits breast cancer in animal models. The objective of the current study was to characterize I3C-induced cell death in a panel of human breast tumorigenic cells (MCF7, MDA-MB-468, MDA-MB-231 and HBL100) in comparison with normal fibroblasts. Since epithelial cells are protected from cell death by a three-dimensional environment, 3D cell culture (collagen I gel and spheroids) was employed to investigate susceptibility to I3C. Cell viability in the presence of 256 μM I3C, a concentration close to the physiologically achievable range, was in the order fibroblasts=HBL100>MDA-MB-231>MCF7>MDA-MB-468 in monolayer culture. However, 3D culture conditions increased the susceptibility of MCF7 and MDA-MB-468 cancer cells towards I3C. I3C induced cell death in breast cancer MCF7, MDA-MB-468 and MDA-MB–231 cells via the mitochondrial apoptotic pathway. I3C significantly reduced levels of epidermal growth factor receptor (EGFR) in MDA-MB-468 after 6 h and in MDA-MB-231 and HBL100 cells after 30h. Downregulation of EGFR in MDA-MB468 and MDA-MB-231 cells using an EGFR inhibitor resulted in apoptosis. EGFR modulation using EGF or an EGFR inhibitor markedly influenced viability and response to I3C in MDA-MB-468 cells in 3D conditions. EGFR expression was modulated by 3D conditions. Therefore, I3C-induced EGFR reduction in these cells is likely to be responsible for I3C-induced apoptosis.

Keywords: indole-3-carbinol, breast cancer, 3D cell culture, apoptosis, epidermal growth factor receptor.

Introduction

Breast cancer has the highest incidence in women in the Western world compared to other forms of cancer. In England and Wales, the number of breast cancer cases between 1988-1990 exceeded the number of cases of lung and colon cancer taken together.[1] Current estimates indicate that one in eight women will be diagnosed with breast cancer in her lifetime. Epidemiological studies and analysis of diet suggest that consumption of some foods, e.g. those containing genistein, coincides with the reduced risk of breast cancer.[2, 3]

Indole-3-carbinol (I3C), derived from vegetables of the Cruciferae family, such as broccoli, brussel sprouts and cabbage, has been shown to inhibit development of tumors in a variety of tissues in animal models (thoroughly reviewed in [4]). It reduces or delays development of mammary tumors induced by carcinogens and viruses, as well as growth of spontaneous mammary tumors in animal models. Therefore, it is regarded as a promising chemopreventive agent. Two clinical phase II trials indicated that I3C causes significant regression of cervical intraepithelial neoplasia and recurrent respiratory papillomatosis in patients.[5, 6]

The chemopreventive efficacy of I3C can be partially attributed to its effect on estradiol metabolism, since it increases 2-hydroxylation and decreases proliferative activity of endogenous estrogens in volunteers and patients, as well as in animal models.[4, 5, 7, 8] However, both estrogen receptor (ER)-negative MDA-MB-231 and MDA-MB-468 cells and ER-positive MCF7 breast cancer cells are affected by I3C. I3C has been reported to inhibit growth of MDA-MB-231 cells and induce apoptosis in MDA-MB-468 and MCF7 cells.[9-13] Therefore, the mechanisms of I3C-induced growth inhibition or apoptosis are not related to ER status and remain obscure.

Data on the mechanism of I3C-induced apoptosis are contradictory. I3C-induced apoptosis was related to increased death receptors, DR4 and DR5, in prostate cancer LNCaP cells, which points to an extrinsic apoptotic pathway.[14] Conversely, upregulation of pro-

apoptotic Bax and downregulation of anti-apoptotic Bcl-2 and Bcl-xL preceded or coincided with the onset of apoptosis in prostate cancer PC3 and breast cancer MDA-MB-435 cells.[15-17] These data imply involvement of an intrinsic apoptotic pathway. There is also some confusion regarding the sequence of apoptotic events induced by I3C. Loss of mitochondrial membrane potential and cytochrome release preceded downregulation of Bcl-2 and translocation of Bax into mitochondria in breast cancer cells MCF10CA1a.[18] In breast cancer cells MDA-MB-468, modulation of Bcl-xL and Bcl-2 occurred as post-apoptotic events. [13] Furthermore, several studies showed that I3C upregulates expression of pro-apoptotic proteins, e.g. DR4, DR5, caspase-1 and Bax, at transcriptional and protein levels.[14-16,19].Therefore, we investigated which initiator caspase was involved in the apoptotic pathway in breast cancer cells in more detail. We also examined epidermal growth factor receptor (EGFR), which is required for maintaining viability of EGFR-dependent solid tumours[20], as a primary I3C target. EGFR signaling plays an important role in cancer development and progression.[21]

Cells in tissues are involved in three-dimensional interactions, and it is well known that their physiology and fate is influenced by a 3D environment. Modulation of cell adhesion in laminin-based 3D culture dramatically influences morphology and function of breast cancer cells.[22, 23] Laminin-based and spheroid 3D cultures protect some breast cells from apoptosis or increase resistance to cytotoxic agents compared to monolayer culture. [24-26] The aim of this study was to investigate whether 3D culture altered the susceptibility of breast cancer cells to I3C. Collagen-based 3D culture is more relevant for our investigation, because breast cancer is associated with basement membrane fragmentation, increased collagen synthesis and accumulation.[23, 27] Aggressive breast cancer induces a strong fibroproliferative response with synthesis of type I collagen.[28] Metastatic spreading of breast cancer cells *in vivo* occurs along collagen filaments.[29] Moreover, drug resistance tests using collagen gel culture have proved to be accurate and highly predictive.[30, 31] All cell lines used in this study express $\alpha 2\beta 1$ integrin, [32] responsible for adhesion to collagen I. The other 3D model we

investigated was spheroid culture, because in some cases cells in spheroids are more resistant to cytotoxic agents than in monolayer culture.[25, 26] For these reasons, we compared the effect of I3C on breast cells grown in monolayers and in two 3D models.

We investigated I3C-induced cell death in human breast cancer cells in comparison to the transformed breast cell line HBL100 and normal fibroblasts. A panel of cancer cell lines (MCF7, MDA-MB-468 and MDA-MB-231) was chosen to represent cells with a wide range of tumorigenicity. They produce tumors in nude mice with efficiencies of 22, 90 and 100%, and are known as non-metastatic, poorly metastatic and aggressively metastatic, respectively.[33,34] The breast cell line HBL100, derived from normal human breast epithelium and containing integrated defective SV40 virus, was also included in the study. This transformed cell line is able to form colonies in soft agar and produce adenocarcinomas in nude mice.[35,36]

Methods

Cells

Human breast cell lines MCF7 (ER^{+ve}, $p53^{wt}$), MDA-MB-468 (ER^{-ve}, $p53^{mutated}$), MDA-MB-231 (ER^{-ve}, $p53^{mutated}$) and HBL100 (ER^{-ve}, $p53^{wt}$), originating from the American Type Culture Collection, were kindly provided by Prof. Rosemary Walker (University of Leicester, UK). All cells were cultured in as described previously.[32] Normal human fibroblasts GM05399 were obtained from Coriell Cell Repositories (Camden, NJ, USA) and used in passages 12-16. For culture in collagen gels, collagen I (Invitrogen) was diluted in DMEM to the concentration of 1 mg/ml (on ice), the pH adjusted to within physiological range, mixed with cells and dispensed in Packard Viewplates-96 (2500 cells/100 μl per well). After 1 h incubation at 37°C to set collagen gels, an equal volume of the medium containing 20% FBS was added. In some experiments an equal amount (1 mg/ml) of growth factor-reduced matrigel (BD Biosciences) was added to collagen I before mixing with cells. Spheroids were generated by seeding 2.5 x 10^4 cells/ml on to 0.8% agarose-coated 24-well tissue culture

plates and overnight incubation. The DMSO amounts were equal in all wells in all experiments and did not exceed 0.1%.

Cell viability and apoptosis-related studies

The viability of cells in response to I3C was determined by measuring ATP levels, since this assay detects the number of cells in a wide range from $5x10^1$ to $5x10^5$. The number of adherent cells was examined using the ATPlite kit (Perkin-Elmer), according to the manufacturer's recommendations, in a FluoStar plate-reader (BMG). Cells were seeded in white Packard Viewplates-96 (2500 cells/well) overnight in DMEM containing 10% FBS, followed by I3C treatment in the same medium for 48 h.

The following adjustments were made for 3D cultures. To measure ATP levels in cells grown in collagen gels, time periods for cell extraction and ATP assay were extended from 15 min to 90 min to obtain the highest measurements. Formed spheroids were treated with I3C for 48 h and transferred to Packard Viewplate-96 plates in aliquots/well, equivalent to 2.5 x 10^3 cells of the starting spheroid culture, for measuring ATP amounts as described above. In some experiments cells were treated with a highly specific EGFR inhibitor PD153035 (Calbiochem, UK) or EGF (Sigma).

Apoptosis was measured using the Annexin V-FITC kit (Bender Medsystems) as described previously[13]. The percentage of live, apoptotic or necrotic cells in the whole population was determined using a FACScan flow cytometer. In some experiments cycloheximide (Sigma), Z-YVAD-FMK (Sigma) or Z-VAD-FMK (Promega) was added to the cell culture medium 60 min prior to I3C. The effect of I3C on mitochondrial potential was measured via tetramethylrhodamine ethyl ester (TMRE) binding to I3C-treated adherent cells using a FACScan flow cytometer as described previously.[37] TMRE is a cationic lipophilic dye that accumulates in the negatively charged mitochondrial matrix.

Caspase activity

Caspase-8 and -9 proteolytic activities were measured using colorimetric protease assays (Biosource) with specific substrates IETD-pNA and LEHD-pNA, respectively. Protein lysates (100 μg) of adherent MDA-MB-468 cells were processed according to the manufacturer's instructions. Absorbance of free chromophore pNA was quantified at 405 nm in the Fluostar plate-reader. Data are presented as a percentage of activity of non-induced controls after subtraction of negative controls without the specific substrate.

Caspase-3/7 activity was measured using Caspase-Glo 3/7 kit (Promega) according to the manufacturer's instructions. Cells were seeded in white Packard Viewplates-96 (10000 cell/well) overnight in 10% FBS in DMEM, followed by treatments in the same medium. Luminescence was detected in the Fluostar plate-reader 40 min after addition of luminogenic substrate containing Z-DEVD sequence specific for caspases-3 and/or -7. Data are presented as fold increase in luminescence of treated samples.

Protein analysis

Preparation of cell lysates, SDS-PAGE and immunoblotting were performed according to standard procedures.[38] Briefly, cells were extracted with a triple detergent buffer, containing inhibitors for proteases and phosphotyrosine and phosphoserine / phosphothreonine phosphatases (all cocktails from Sigma). Protein concentrations were measured using the Bio-Rad protein assay. Proteins were separated by SDS-PAGE, blotted onto nitrocellulose filters, incubated with primary antibodies followed by the secondary antibody conjugated to HRP (Dako) and detected with ECL or ECLplus (EGFR in HBl100 and MCF7 cells) reagent (Amersham). Western blots were routinely probed with several primary antibodies. Antibodies used in this study were against: EGFR (monoclonal R19/48, polyclonal pY845 and pY1068 from Biosource), Erk (monoclonal sc-7383 pErk and polyclonal sc-94 Erk-1 from Santa Cruz Biotechnology), Akt (polyclonal pS473 from

Biosource; Akt-1 C-20 from Santa Cruz Biotechnology), β-actin (polyclonal from Sigma), N-cadherin (monoclonal 32; BD transduction laboratories), E-cadherin (monoclonal AF748; R&D Systems), β1-integrin (polyclonal sc-8978 from Santa Cruz Biotechnology). Protein bands on exposed films were quantified using a Syngene image system.

Data analysis

Differences among the groups were analyzed using one-way ANOVA in Statistical Package for the Social Sciences, followed by Scheffe's test to determine whether the treatment groups were different, or by Dunnett's test to determine whether the treatment groups were different from a control group. $P < 0.05$ was selected as the level of statistical significance.

Results

I3C-induced apoptosis

I3C caused apoptosis in MDA-MB-468 and MDA-MB-231 cells and necrosis in MCF7 cells after 24h treatment with 256 μM I3C (Fig. 1A), which is close to a physiologically achievable range, identified recently by Anderton et al, who detected I3C ranging from 40 to 170 μM in several mouse tissues after a single dose administration.[39] After 48 hours, I3C further increased cell death in MCF7, MDA-MB-468 and MDA-MB-231 cells (Fig. 1B). Increased necrosis in MDA-MB-468 and MDA-MB-231 cells after 48h treatments is likely to be secondary to apoptosis and a consequence of further disintegration of apoptotic cells. Cell death in the presence of 256 μM I3C in this assay was in the order MDA-MB-231<MCF7<MDA-MB-468. In contrast to cancer cells, transformed HBL100 cells underwent necrosis only at a non-physiological concentration of 512 μM.

Significantly increased activity of effector caspases 3/7 was found after 30 h of I3C treatments in MDA-MB468 and MDA-MB-231, but not HBL100 or MCF7 cells (Fig. 2 A).

The levels of the effector caspase activity correlated with the levels of apoptosis, detected by annexin V binding, observed in these cells (Fig. 1). MCF7 cells possess a non-functional caspase-3 gene.[40] In agreement with this, no increase in caspase3/7 activity nor phosphatidylserine externalisation was observed in MCF7 cells despite significant I3C-induced loss of viability. I3C-induced activation of effector caspases did not require protein synthesis (Fig. 2B). In fact, inhibition of protein synthesis during I3C treatment enhanced activation of caspases in MDA-MB-468 cells and induced activation in HBL100 cells, which did not develop apoptosis after the treatment with I3C alone.

The apoptotic process in the most susceptible cells, MDA-MB-468, was investigated in detail. I3C-induced apoptosis was significantly reduced by a pan-caspase inhibitor Z-VAD-FMK, but not by a caspase-1-specific inhibitor Z-YVAD-FMK (Fig. 3). The mRNA level of caspase-1 was not changed in the presence of I3C (not shown). Treatment with 125 μM I3C induced loss of mitochondrial membrane potential after 20 h treatment (Fig. 4A). Two-fold activation of an initiator caspase-9 was observed after 20 h treatment followed by weak activation of caspase-8 after 24 h (Fig. 4B). Activity of effector caspases 3/7 was increased by 2 fold after 24 h of treatment with 125 μM I3C (Fig. 4C). Apoptosis, measured using phosphatidylserine externalisation dependent on caspase-3 activity [41], was detected starting from 24 h of treatment (Fig. 4D). Taken altogether, these data implied that I3C induced caspase-dependent apoptosis, initiated by the loss of mitochondrial membrane potential and activation of the initiator caspase-9, followed by activation of effector caspases 3/7 and phosphatidylserine externalisation. This sequence of events is indicative of the mitochondrial apoptotic pathway. Since MCF7 cells do not display typical features of apoptosis, we investigated whether I3C affected mitochondrial membrane potential in these cells. I3C induced significant loss of mitochondrial membrane potential in a time-dependent manner (Fig. 5A) similar to MDA-MB-468 cells. The rate of loss of membrane potential exceeded the rate of decreasing viability in these cells (Fig. 5B). Therefore, we concluded that I3C-induced

cell death in all cancer cells proceeded via the mitochondrial apoptotic pathway, although the absence of functional caspase-3 in the MCF7 cells prevented the final apoptotic outcome.

Effect of the 3D environment on susceptibility of breast cancer cells to I3C

Viability of cells grown as monolayers on plastic was reduced by I3C in the concentration range of 128-256 μM (Table 1) with susceptibility to 256 μM I3C in the same order (HBL100<MDA-MB-231<MCF7<MDA-MB-468), as determined by measuring apoptosis. The MDA-MB-231 and MCF7 cells were slightly more resistant to 512 μM I3C compared to HBL100 cells. MDA-MB-468 cells were two-four times more susceptible to I3C compared to other cell types.

Collagen gel culture significantly increased the viability of transformed HBL100 cells in the presence of I3C (Table 1), conferring resistance to 256 μM in a 3D environment. On the contrary, the cancer cells MCF7 and MDA-MB-468 in collagen culture exhibited lower viability in the presence of 32-256 μM I3C compared to that on plastic. Addition of basement membrane (matrigel) proteins to collagen I gels did not affect I3C susceptibility of MDA-MB-468 cells compared to that of collagen I gel (not shown). I3C inhibited MDA-MB-468 cell growth in both types of gel to a greater extent than in monolayer culture. Interestingly, MCF7 cells were more resistant to 512 μM I3C compared to HBL100 cells in collagen gel culture. The susceptibility of the aggressive metastatic cell line MDA-MB-231 was not affected by culturing in collagen gel. The susceptibility of breast cells grown in collagen gel in the presence of 256 μM I3C was in the order MDA-MB-231<MCF7<MDA-MB-468.

Viability of transformed HBL100 cells grown as spheroids in the presence of 128-512 μM I3C was dramatically increased compared to that of a monolayer. A small increase in viability of MCF7 cells in spheroids was observed only in the presence of 512 μM I3C. MDA-MB-468 spheroids were more susceptible to the presence of 128-256 μM than cells grown on plastic. The sensitivity of the metastatic MDA-MB-231 cells was not affected by

128-512 μM I3C when cultured as spheroids, but was increased in response to 32-64 μM I3C. The susceptibility in spheroid cultures to 256 μM I3C was in the same order as that in collagen gel culture.

Altogether these results indicated that 3D culturing conditions could affect susceptibility of cells to I3C, when compared with monolayers, decreasing viability of MCF7 and MDA-MB-468 cells in the presence of 32-256 μM I3C. In contrast, viability of the transformed HBL100 cells in the presence of I3C in both 3D cultures was significantly increased compared with that in a monolayer on plastic. In fact, HBL100 cells were resistant to 128-256 μM I3C in 3D culturing conditions, whereas all cancer cells were susceptible to these concentrations. MDA-MB-468 cells in all culturing conditions were significantly more susceptible to 128-256 μM of I3C compared to other cell lines. The sensitivity of the aggressively metastatic cell line MDA-MB-231 was mostly unaffected by 3D culturing conditions, although a small increase in susceptibility to low I3C concentrations was observed in spheroids.

The effect of I3C on normal human fibroblasts was also investigated. I3C did not induce activity of caspase3/7 in fibroblasts (Fig. 6A), but caused necrosis in a small proportion of fibroblasts (Fig. 6B). Their viability in a monolayer was slightly decreased by 512 μM I3C (Fig. 6C). Fibroblasts grown in collagen gel were more susceptible to 384-512 μM I3C compared to a monolayer culture (Fig. 6C). However, the fibroblasts were much more resistant to I3C compared to tumorigenic cells (compare Fig. 6 and Table 1). They did not form spheroids, as no live cells survived following overnight suspension. Collectively, these data indicated that the fibroblasts were significantly less susceptible to I3C compared to tumorigenic cells.

EGFR is involved in I3C induced cell death

The mitochondrial apoptotic pathway is inhibited by growth factors. EGFR is overexpressed in MDA-MB-468 and MDA-MB-231 cells [42,43], which undergo apoptosis in response to I3C [44]. For these reasons we investigated whether I3C might affect EGFR signaling. I3C treatment of MDA-MB-468 cells resulted in increased phosphorylation (163%) of the activation loop of EGFR (Y845) after 6 h, increased autophosphorylation (Y1068, 128-123%) and reduced EGFR expression (82-71%) after 6-12h of I3C treatment (Fig. 7A and 7C). I3C-induced EGFR activation resulted in increased Erk signalling (181-172%) at 6-12h. EGFR levels were restored after 18-30h of I3C treatment in MDA-MB-468 cells (Fig. 7D); however, the apoptotic program was already switched on at that time (Fig. 4). No changes in EGFR levels were detected in other cells during 6-12h of I3C treatment (Fig. 7B), but reductions in EGFR expression were detected after 24-30h in MDA-MB-231 and HBL100 cells (Fig. 7D and 7E). After 30h treatment, EGFR levels decreased to 30 and 31 % in HBL100 and MDA-MB-231 cells, respectively. The low EGFR level in MCF7 cells made any reliable estimation of the changes impossible. (EGFR expression in MCF7 cells could only be observed using the most sensitive detection conditions) No changes in Akt signaling or expression of cell-cell adhesion receptors cadherins or β-catenin (not shown) were observed in any cell line during I3C treatments.

Since I3C-induced EGFR downregulation was detected in three out of four tested tumorigenic cell lines, we investigated whether downregulation of EGFR function was responsible for cell death using a specific EGFR tyrosine kinase inhibitor PD153035. The inhibitor induced activation of caspase-3/7 activity in MDA-MB-468, MDA-MB-231 (5-20 μM) and HBL100 (10-20 μM) cells and reduced it in human fibroblasts (10-20 μM) (Fig. 8A). EGFR inhibitor PD153035 reduced viability of MDA-MB-468 (5-20 μM), MDA-MB-231, MCF7 and human fibroblasts (10-20 μM), but not HBL100 cells (Fig. 8B). MDA-MB-468 and MDA-MB–231 cells were particularly sensitive to inhibition of EGFR signaling;

therefore, I3C-induced downregulation of EGFR in these cells, but not in HBL100 cells, is likely to be responsible for caspase activation and apoptosis.

There is a body of evidence on the role of EGFR in cell adhesion (see Discussion section); hence, we investigated whether EGFR modulated I3C-induced cell death in MDA-MB-468 cells in 3D conditions. EGFR was either stimulated by EGF or inhibited by 100 nM PD153035, which did not affect cell viability. EGF stimulation, but not the EGFR inhibitor, reduced cell viability and further increased cell death in the presence of I3C in monolayer culture (Fig. 9A). In collagen culture, both EGF and EGFR inhibitor significantly reduced cell viability and I3C did not increase cell death in the presence of EGF or EGFR inhibitor probably due to a low viability level in the presence of I3C in collagen (Fig. 9B). EGF significantly increased cell number in spheroid culture in contrast to that in monolayer or collagen, however, the EGFR inhibitor reduced cell viability in spheroids similarly to that in collagen (Fig. 9C). I3C still reduced viability, while EGF increased cell proliferation in spheroids in the presence of I3C. The combination of the EGFR inhibitor with I3C almost completely eliminated cells. Protein analysis demonstrated that expressions of EGFR, β1integrin and actin were affected by 3D conditions (Fig. 9D and 9E). Actin expression was increased in 3D conditions. EGFR was present in two forms 170 and 140 kDa in monolayer and collagen cultures, but only as 170 kDa in spheroids. Collagen culture significantly decreased EGFR levels. β1Integrin was expressed as several isoforms with different dominant isoforms in each type of culture. These experiments further support EGFR involvement in the viability of cancer in a 3D environment and the I3C-induced response.

Discussion

Comparison of breast tumorigenic cells with normal fibroblasts showed that normal tissue-derived cells are much more resistant to I3C compared to tumorigenic cells. Similarly normal cells have shown greater resistance to other dietary phytochemicals, such as EGCG

and curcumin. [45,46] Cell viability in the presence of 256 μM I3C was in the order fibroblasts=HBL100>MDA-MB-231>MCF7>MDA-MB-468. Our data indicate that I3C induced cell death in breast cancer cells at concentrations close to the physiologically achievable range. I3C-induced cell death was initiated by the loss of mitochondrial membrane potential, followed by development of the apoptotic program, which was unable to proceed in the normal way in MCF7 cells due to the lack of functional caspase-3. I3C-induced cell death in cancer cells should be distinguished from necrosis in transformed HBL100 cells and normal fibroblasts, caused by cytotoxicity of non-physiological high I3C concentrations. Our data, which are in agreement with the levels of I3C-induced apoptosis in MDA-MB-468, HBL100 and MCF7 cells[12,13], now provide a mechanism involving signaling from EGFR via mitochondrial pathway.

Since I3C has been reported to upregulate expression of pro-apoptotic proteins, e.g. DR4, DR5, caspase-1 and Bax, at transcriptional and protein levels in various cell types [14-16, 19], we investigated if I3C-induced apoptosis requires protein synthesis. Inhibition of protein synthesis with cycloheximide did not reduce I3C-induced apoptosis. On the contrary, inhibition of protein synthesis increased apoptosis in MDA-MB-468 cells and induced apoptosis in HBL100 cells. In fact, protein synthesis protected HBL100 cell from I3C-induced apoptosis. Because of contradictory reports on the mechanism of I3C-induced apoptosis in different cell types and potential involvement of the initiator caspase-1, we investigated which initiator caspases and apoptotic pathways were involved in MDA-MB-468 cells. Although I3C-induced apoptosis was significantly reduced by a pan-caspase inhibitor ZVAD-FMK, a caspase-1-specific inhibitor did not have any affect. Loss of mitochondrial membrane potential and activation of initiator caspase-9 were the earliest detected apoptotic events followed by activation of effector caspases-3/7 and increased phosphatidylserine externalisation. Similarly, I3C induced significant loss of mitochondrial membrane potential

prior to the loss of cell viability in MCF7 cells. The sequence of I3C-induced events involved a mitochondrial apoptotic pathway in cancer cells.

Further investigation indicated that 3D culturing conditions dramatically influenced I3C susceptibility of all non-metastatic cell lines in this study. The transformed HBL100 cells became resistant to 128-256 μM I3C in 3D conditions, whereas two cancer cell lines, MCF7 and MDA-MB-468, became more susceptible. Interestingly, a similar effect of laminin-based 3D culture on induced cell death has been reported.[24] In that study transformed mammary S-1 cells underwent apoptosis following exposure to several agents in a monolayer, but not in 3D culture. Conversely, tumorigenic T4-2 cells underwent apoptosis in both culturing conditions and were more susceptible to chemically induced apoptosis in 3D culture. β4 Integrin was responsible for modulation of apoptosis in that study. This integrin does not support adhesion to collagen and is not expressed in either MCF7 or MDA-MB-468 cells.[32] Our data indicated that β1integrin was modulated by 3D conditions in MDA-MB-468 cells. Culturing MCF7 cells in collagen gels increased susceptibility to I3C compared to a monolayer, but spheroid formation did not. Nor did spheroids protect these cells from I3C in contrast to reports of protection against other agents.[26] It is noteworthy that MCF7 viability increased in 3D conditions at 512 μM I3C. This raises the possibility that a small proportion of cells would remain viable even at high concentrations of I3C in vivo, despite the majority of population being I3C-sensitive. This implies that additional therapies may be required for certain cancer cell types to eliminate such cancer cells completely

The susceptibility of the metastatic cancer cells MDA-MB-231 was mostly unaffected by culture conditions, although a slight reduction in cell viability of spheroids was detected in the presence of low I3C concentrations. Recent studies indicate that metastatic breast cancer cells express activated αvβ3 integrin, which prevents apoptosis when cell adhesion is impaired, e.g. in blood flow.[47] Therefore, cell viability of metastatic cancer cells may not be influenced by adhesion to the same extent as that of other cancer cells.

The mitochondrial apoptotic pathway is blocked by growth factor signaling in live cells. EGFR is markedly overexpressed in MDA-MB-468 and MDA-MB–231 cells, which undergo I3C-induced apoptosis. Reported levels of EGFR are much higher in MDA-MB-468 ($2x10^6$/cell) and MDA-MB-231 cells ($1\text{-}2x10^5$/cell) compared with HBL100 ($2.5x10^4$/cell) or MCF7 ($2.9x10^3$/cell).[42,43] For these reasons, we investigated EGFR signaling in I3C-treated cells. In MDA-MB-468 cells, I3C induced EGFR activation and autophosphorylation, leading to EGFR degradation as a part of a negative feedback-loop.[21] EGFR activation resulted in increased downstream Erk signaling. EGFR is an important factor in maintaining cell survival. I3C-induced downregulation of EGFR occurred prior to initiation of the apoptotic program in MDA-MB-468 cells. Analysis of EGFR expression indicated that I3C reduced levels also in MDA-MB-231 and HBL100 cells, although the dynamics were different in these cells with downregulation of EGFR occurred much later than in MDA-MB-468 cells. These differences may account for super-sensitivity of MDA-MB-468 cells. Similarly, I3C-induced reduction of EGFR has been reported after 24h in prostate cancer PC3 cells by Sarkar and co-authors.[17] However, I3C-induced apoptosis was attributed to reduction in Akt activation in that study. In contrast, no reduction in Akt activation was observed in our study in any cell line tested at concentrations which induced significant apoptosis, although reduction in pAkt in MDA-MB-468 cells was reported for higher I3C concentrations.[13]

Since inhibition of EGFR signalling with the specific inhibitor PD153035 resulted in activation of effector caspases and significant loss of viability in MDA-MB-468 and MDA-MB-231 cells, I3C-induced reduction of EGFR is likely to have a similar effect. Interestingly, the EGFR inhibitor induced 1.9-fold caspase activation in HBL100 cells, but no significant loss of viability was detected. These cells seem to be resistant to this level of caspase activation. Similarly, I3C-induced reduction in the EGFR did not result in cell death in these cells. Since blocking synthesis of new proteins in I3C-treated HBL100 cells induced apoptosis, it is possible that sustained downregulation of EGFR is required to induce

apoptosis in these cells. The MCF7 cells exhibited some level of sensitivity to EGFR inhibition, but the effect of I3C on EGFR could not be reliably detected in these cells due to extremely low EGFR expression. Hence, involvement of EGFR could not be ruled out completely, particularly because of cross-talk between ER and EGFR pathways in MCF7 cells.[48] Inhibition of EGFR in human fibroblasts resulted in reduced cell numbers without caspase activation, which may be contribute to some of the common side effects observed in patients treated with EGFR inhibitors, such as skin rashes

Modulation of cell viability in collagen gels or spheroids might be related to adhesion receptors, α2β1 integrin and cadherins involved in cell-extracellular matrix (collagen I) interactions or cell-cell interactions, respectively, and would impact differently on the physiology of different cancer cell types. However, no changes in N-cadherin (HBL100 cells), E-cadherin (MCF7 and MDA-MB-468 cells) or cadherin-11 (MDA-MB-231 cells) were observed after I3C treatment or in 3D conditions (MDA-MB-468). On the other hand, a large body of evidence implicates EGFR in cell adhesion, particularly in the 3D environment. EGFR affects cell-extracellular matrix adhesion in breast cancer cells, co-precipitates with cell adhesion receptors integrins and is activated by β1 and αvβ3 integrins.[49,50] Integrin-dependent adhesion in monolayer culture increases EGFR on the cell surface.[49] EGF stimulation resulted in decreased and increased adhesion of MDA-MB-468 and MDA-MD-231 cells, respectively.[51] EGFR regulates assembly of E-cadherin-actin adhesion complexes in MDA-MB-468 cells.[52] Moreover, EGFR is implicated in protection from apoptosis in bladder cancer spheroids.[53] In contrast to integrin-based adhesion, EGFR expression is downregulated in A431 spheroids.[49,54] Interestingly, EGF stimulation induces apoptosis in monolayer culture in several cancer cell lines, including MDA-MB-468 cells.[44]

In MDA-MB-468 cells, expression of several proteins was modulated by 3D conditions. Decreased EGFR expression in collagen gel may account for increased sensitivity to EGF or the EGFR inhibitor, compared to those in monolayer culture. EGFR was expressed

as 170 and 140 kDa bands in monolayer and collagen cultures. The later is likely to present a constitutively active EGFRvIII isoform, which may originate from alternative splicing of the ligand-binding site in the extracellular domain, found in several cancer types including breast cancer [20, 21]. The absence of this particular isoform in spheroids may account for normal response to EGF, e.g. increasing cell numbers. EGF increased viability of MDA-MB-468 spheroids in the presence of I3C; similarly, EGF-induced protection from apoptosis has been reported for bladder cancer spheroids.[53]. In contrast to opposite effects of EGF stimulation in the different 3D cultures, the EGFR inhibitor caused a loss of cell viability in both collagen gels and spheroids. Since EGFR is involved in assembly of both integrin and cadherin complexes, EGFR inhibition may negatively affect formation of cell adhesion complexes in both types of 3D culture and, thereby, decrease cell viability. Therefore, EGFR modulation using either a specific inhibitor or EGF stimulation had a significant effect on the behavior of MDA-MB-468 cells in 3D culture and in the presence of I3C.

Collectively, our data indicated that changes in EGFR expression preceded any other events induced by I3C in MDA-MB-468 cells or coincided with the onset of apoptosis in MDA-MB-231 cells, implicating this receptor in I3C-induced apoptosis in EGFR-dependent breast cancer cells. EGFR-dependence of some lung and colon cancers has been confirmed in recent and ongoing trials with small EGFR tyrosine kinase inhibitors.[20] We have not identified factors involved in I3C-induced death of MCF7 cells; therefore, EGFR cannot be considered as the only biomarker implicated in I3C-induced cancer cell death.

Conclusions

The current study has provided an initial characterization of breast cancer cell types and conditions rendering cells susceptible to I3C. In 3D conditions, I3C, in a physiological range of concentrations, induced cell death and loss of viability only in cancer cells, regardless of their ER status or p53 function, in contrast to its lack of effect in transformed or normal cells. 3D culture abrogated any susceptibility of the transformed cell line HBL100 and

increased resistance of MCF7 cells to high concentrations of I3C. These data imply that some cell types are resistant to I3C or cannot be eliminated completely by treatment with I3C alone, particularly in a 3D environment *in vivo*. Our data show an important role of EGFR in susceptibility to I3C, modulated by cell adhesion in cancer cells. We speculate that malignant EGFR-dependent and some other cancer phenotypes are likely to be susceptible to I3C *in vivo*. Further analysis of prognostic biomarkers and signaling pathways in I3C-sensitive cancer types will provide critical information for identifying cancer types susceptible to I3C and for developing I3C-supplemented anti-cancer therapies or prevention strategies. Use of I3C in combination with other anti-EGFR therapies should be explored in order to gain maximal benefits from anti-EGFR therapy.

Acknowledgements

This work was funded by the UK Medical Research Council Grant No.G0100872. The authors are grateful to Dr E. Ann Hudson for assistance with some data in Fig. 1A.

References

1. Parkin DM, Whelan SL, Storm H. Cancer incidence in five continents. Vol. 7. Lyon: IARC, 2005.
2. Lee HP, Gourley L, Duffy SW, Esteve J, Lee J, Day NE. Dietary effects on breast-cancer risk in Singapore. Lancet 1991; 337: 1197-200.
3. Linseisen J, Piller R, Hermann S, Chang-Claude J. Dietary phytoestrogen intake and premenopausal breast cancer risk in a German case-control study. Int J Cancer 2004; 110: 284-90.
4. IARC. Cruciferous vegetables, isothiocyanates and indoles. IARC Handbooks of Cancer Prevention. Lion: IARC Press, 2004, Vol. 9, pp. 1-262..
5. Bell MC, Crowley-Nowick P, Bradlow HL, et al. Placebo-controlled trial of indole-3-carbinol in the treatment of CIN. Gynecol Oncol 2000; 78: 123-9.

6. Rosen CA, Bryson PC. Indole-3-carbinol for recurrent respiratory papillomatosis: long-term results. J Voice 2004; 18: 248-53.

7. Bradlow HL, Michnovicz J, Telang NT, Osborne MP. Effects of dietary indole-3-carbinol on estradiol metabolism and spontaneous mammary tumors in mice. Carcinogenesis 1991; 12: 1571-4.

8. Kojima T, Tanaka T, Mori H. Chemoprevention of spontaneous endometrial cancer in female Donryu rats by dietary indole-3-carbinol. Cancer Res 1994; 54: 1446-9.

9. Tiwari RK, Guo L, Bradlow HL, Telang NT, Osborne MP. Selective responsiveness of human breast cancer cells to indole-3-carbinol, a chemopreventive agent. J Natl Cancer Inst 1994; 86: 126-31.

10. Telang NT, Katdare M, Bradlow HL, Osborne MP, Fishman J. Inhibition of proliferation and modulation of estradiol metabolism: novel mechanisms for breast cancer prevention by the phytochemical indole-3-carbinol. Proc Soc Exp Biol Med 1997; 216: 246-52.

11. Cover CM, Hsieh SJ, Tran SH, et al. Indole-3-carbinol inhibits the expression of cyclin-dependent kinase-6 and induces a G1 cell cycle arrest of human breast cancer cells independent of estrogen receptor signaling. J Biol Chem 1998; 273: 3838-47.

12. Ge X, Fares FA, Yannai S. Induction of apoptosis in MCF-7 cells by indole-3-carbinol is independent of p53 and Bax. Anticancer Res 1999; 19: 3199-203.

13. Howells LM, Gallacher-Horley B, Houghton CE, Manson MM, Hudson EA. Indole-3-carbinol inhibits protein kinase B/Akt and induces apoptosis in the human breast tumor cell line MDA MB468 but not in the nontumorigenic HBL100 line. Mol Cancer Ther 2002; 1: 1161-72.

14. Jeon KI, Rih JK, Kim HJ, et al. Pretreatment of indole-3-carbinol augments TRAIL-induced apoptosis in a prostate cancer cell line, LNCaP. FEBS Lett 2003; 544: 246-51.

15. Rahman KM, Aranha O, Glazyrin A, Chinni SR, Sarkar FH. Translocation of Bax to mitochondria induces apoptotic cell death in indole-3-carbinol (I3C) treated breast cancer cells. Oncogene 2000; 19: 5764-71.

16. Chinni SR, Li Y, Upadhyay S, Koppolu PK, Sarkar FH. Indole-3-carbinol (I3C) induced cell growth inhibition, G1 cell cycle arrest and apoptosis in prostate cancer cells. Oncogene 2001; 20: 2927-36.

17. Chinni SR, Sarkar FH. Akt inactivation is a key event in indole-3-carbinol-induced apoptosis in PC-3 cells. Clin Cancer Res 2002; 8: 1228-36.

18. Sarkar FH, Rahman KM, Li Y. Bax translocation to mitochondria is an important event in inducing apoptotic cell death by indole-3-carbinol (I3C) treatment of breast cancer cells. J Nutr 2003; 133: 2434S-2439S.

19. Ashok BT, Chen YG, Liu X, et al. Multiple molecular targets of indole-3-carbinol, a chemopreventive anti-estrogen in breast cancer. Eur J Cancer Prev 2002; 11: S86-93.

20. Gazdar AF, Shigematsu H, Herz J, Minna JD. Mutations and addiction to EGFR: the Achilles 'heal' of lung cancers? Trends Mol Med 2004; 10: 481-6.

21. Laskin JJ, Sandler AB. Epidermal growth factor receptor: a promising target in solid tumours. Cancer Treat Rev 2004; 30: 1-17.

22. Weaver VM, Petersen OW, Wang F, et al. Reversion of the malignant phenotype of human breast cells in three-dimensional culture and in vivo by integrin blocking antibodies. J Cell Biol 1997; 137: 231-45.

23. Gudjonsson T, Ronnov-Jessen L, Villadsen R, Rank F, Bissell MJ, Petersen OW. Normal and tumor-derived myoepithelial cells differ in their ability to interact with luminal breast epithelial cells for polarity and basement membrane deposition. J Cell Sci 2002; 115: 39-50.

24. Weaver VM, Lelievre S, Lakins JN, et al. beta4 integrin-dependent formation of polarized three-dimensional architecture confers resistance to apoptosis in normal and malignant mammary epithelium. Cancer Cell 2002; 2: 205-16.

25. Durand RE, Olive PL. Resistance of tumor cells to chemo- and radiotherapy modulated by the three-dimensional architecture of solid tumors and spheroids. Methods Cell Biol 2001; 64: 211-33.

26. dit Faute MA, Laurent L, Ploton D, Poupon MF, Jardillier JC, Bobichon H. Distinctive alterations of invasiveness, drug resistance and cell-cell organization in 3D-cultures of MCF-7, a human breast cancer cell line, and its multidrug resistant variant. Clin Exp Metastasis 2002; 19: 161-8.

27. Guo YP, Martin LJ, Hanna W, et al. Growth factors and stromal matrix proteins associated with mammographic densities. Cancer Epidemiol Biomarkers Prev 2001; 10: 243-8.

28. Jensen BV, Johansen JS, Skovsgaard T, Brandt J, Teisner B. Extracellular matrix building marked by the N-terminal propeptide of procollagen type I reflect aggressiveness of recurrent breast cancer. Int J Cancer 2002; 98: 582-9.

29. Wang W, Wyckoff JB, Frohlich VC, et al. Single cell behavior in metastatic primary mammary tumors correlated with gene expression patterns revealed by molecular profiling. Cancer Res 2002; 62: 6278-88.

30. Tanino H, Oura S, Hoffman RM, et al. Acquisition of multidrug resistance in recurrent breast cancer demonstrated by the histoculture drug response assay. Anticancer Res 2001; 21: 4083-6.

31. Takamura Y, Kobayashi H, Taguchi T, Motomura K, Inaji H, Noguchi S. Prediction of chemotherapeutic response by collagen gel droplet embedded culture-drug sensitivity test in human breast cancers. Int J Cancer 2002; 98: 450-5.

32. Gordon LA, Mulligan KT, Maxwell-Jones H, Adams M, Walker RA, Jones JL. Breast cell invasive potential relates to the myoepithelial phenotype. Int J Cancer 2003; 106: 8-16.

33. Biscardi JS, Belsches AP, Parsons SJ. Characterization of human epidermal growth factor receptor and c-Src interactions in human breast tumor cells. Mol Carcinog 1998; 21: 261-72.

34. Zhang RD, Fidler IJ, Price JE. Relative malignant potential of human breast carcinoma cell lines established from pleural effusions and a brain metastasis. Invasion Metastasis 1991; 11: 204-15.

35. Gaffney EV. A cell line (HBL-100) established from human breast milk. Cell Tissue Res 1982; 227: 563-8.

36. Caron de Fromentel C, Nardeux PC, Soussi T, et al. Epithelial HBL-100 cell line derived from milk of an apparently healthy woman harbours SV40 genetic information. Exp Cell Res 1985; 160: 83-94.

37. Gottlieb E, Vander Heiden MG, Thompson CB. Bcl-x(L) prevents the initial decrease in mitochondrial membrane potential and subsequent reactive oxygen species production during tumor necrosis factor alpha-induced apoptosis. Mol Cell Biol 2000; 20: 5680-9.

38. Sambrook J, Russell DW. Molecular Cloning, 3rd edition. Cold Spring Harbor, New York: Cold Spring Harbor Laboratory Press, 2001.

39. Anderton MJ, Manson MM, Verschoyle RD, et al. Pharmacokinetics and tissue disposition of indole-3-carbinol and its acid condensation products after oral administration to mice. Clin Cancer Res 2004; 10: 5233-41.

40. Janicke RU, Sprengart ML, Wati MR, Porter AG. Caspase-3 is required for DNA fragmentation and morphological changes associated with apoptosis. J Biol Chem 1998; 273: 9357-60.

41. Martin SJ, Finucane DM, Amarante-Mendes GP, O'Brien GA, Green DR. Phosphatidylserine externalization during CD95-induced apoptosis of cells and cytoplasts requires ICE/CED-3 protease activity. J Biol Chem 1996; 271: 28753-6.

42. Fitzpatrick SL, LaChance MP, Schultz GS. Characterization of epidermal growth factor receptor and action on human breast cancer cells in culture. Cancer Res 1984; 44: 3442-7.

43. Ennis BW, Valverius EM, Bates SE, et al. Anti-epidermal growth factor receptor antibodies inhibit the autocrine-stimulated growth of MDA-468 human breast cancer cells. Mol Endocrinol 1989; 3: 1830-8.

44. Armstrong DK, Kaufmann SH, Ottaviano YL, et al. Epidermal growth factor-mediated apoptosis of MDA-MB-468 human breast cancer cells. Cancer Res 1994; 54: 5280-3.

45. Ramachandran C, You W. Differential sensitivity of human mammary epithelial and breast carcinoma cell lines to curcumin. Breast Cancer Res Treat 1999; 54: 269-78.

46. Ahmad N, Gupta S, Mukhtar H. Green tea polyphenol epigallocatechin-3-gallate differentially modulates nuclear factor kappaB in cancer cells versus normal cells. Arch Biochem Biophys 2000; 376: 338-46.

47. Felding-Habermann B, O'Toole TE, Smith JW, et al. Integrin activation controls metastasis in human breast cancer. Proc Natl Acad Sci U S A 2001; 98: 1853-8.

48. Osborne CK, Shou J, Massarweh S, Schiff R. Crosstalk between estrogen receptor and growth factor receptor pathways as a cause for endocrine therapy resistance in breast cancer. Clin Cancer Res 2005; 11: 865s-70s.

49. Moro L, Dolce L, Cabodi S, et al. Integrin-induced epidermal growth factor (EGF) receptor activation requires c-Src and p130Cas and leads to phosphorylation of specific EGF receptor tyrosines. J Biol Chem 2002; 277: 9405-14.

50. Bill HM, Knudsen B, Moores SL, et al. Epidermal growth factor receptor-dependent regulation of integrin-mediated signaling and cell cycle entry in epithelial cells. Mol Cell Biol 2004; 24: 8586-99.

51. Genersch E, Schneider DW, Sauer G, Khazaie K, Schuppan D, Lichtner RB. Prevention of EGF-modulated adhesion of tumor cells to matrix proteins by specific EGF receptor inhibition. Int J Cancer 1998; 75: 205-9.

52. Hazan RB, Norton L. The epidermal growth factor receptor modulates the interaction of E-cadherin with the actin cytoskeleton. J Biol Chem 1998; 273: 9078-84.

53. Dangles V, Femenia F, Laine V, et al. Two- and three-dimensional cell structures govern epidermal growth factor survival function in human bladder carcinoma cell lines. Cancer Res 1997; 57: 3360-4.

54. Mansbridge JN, Ausserer WA, Knapp MA, Sutherland RM. Adaptation of EGF receptor signal transduction to three-dimensional culture conditions: changes in surface receptor expression and protein tyrosine phosphorylation. J Cell Physiol 1994; 161: 374-82.

Table 1. Effect of indole-3-carbinol on cell viability

Cell line	μM I3C / Conditions	0	32	64	128	256	512
MDA-MB-468	Monolayer	100±5.5	103.8±5.8	85.8±4.1	44.3±2.8*	9.4±0.5*	
	Col I	100±3.9	88.2±6.0	35.9±3.0*/#	7.2±1.3*/#	1.2±0.5*/#	0.7±0.1
	Spheroids	100±19.4	125.9±20.6	64.2±11.8	16.8±4.3*/#	3.5±0.8*/#	
MCF7	Monolayer	100±4.2	105.7±6.5	94.8±6.1	74.9±3.4*	33.0±3.0*	8.4±0.8*
	Col I	100±2.5	80.1±3.9*/#	52.4±5.0*/#	40.2±2.4*/#	21.4±1.7*/#	13.8±0.7*/#
	Spheroids	100±9.1	103.4±10.1	73.7±8.9	65.2±7.1*	23.6±1.8*	12.1±1.5*/#
MDA-MB-231	Monolayer	100±6.2	95.1±2.3	95.4±3.5	75.7±3.28*	48.3±1.9*	8.5±0.5*
	Col I	100±5.6	93.1±4.8	93.6±6.6	69.1±4.7*	45.5±3.1*	4.2±0.3*
	Spheroids	100±10.7	67.4±9.1#	67.3±9.0#	56.9±8.8*	42.5±8.0*	8.6±3.1*
HBL100	Monolayer	100±3.6		89.8±2.9	74.6±2.0*	58.6±2.8*	2.8±0.3*
	Col I	100±2.7	86.0±3.7	87.6±4.4	104.4±5.1#	111.1±5.4#	0.5±0.1*
	Spheroids	100±18.0		84.3±8.4	80.6±11.6	101.5±8.8#	25.8±3.0*/#

Data are presented as percentage of means ±SE. The effect of I3C or culturing conditions was analyzed using one-way Anova, Scheffe's test. *, $P<0.05$ versus control cells grown in the absence of I3C. #, $P<0.05$ versus control cells, grown on plastic, with the same treatment. N=16 for monolayer and Col I gel cultures, N=8 for spheroids.

Figure legends

Fig. 1. I3C induced necrosis in HBL100 and MCF7 cells and apoptosis in MDA-MB-468 and MDA-MB-231 cells.

The percentage of live, apoptotic and necrotic cells in the populations was measured after 24 h and 48 h of treatment with I3C (μM). All data are presented as percentage of means ±SD. *, P<0.05 (n=4) compared to "no I3C".

Fig. 2. I3C induced activation of caspase 3/7 activity in MDA-MB-468 and MDA-MB-231 cells, but not in HBL100 or MCF7 cells.

A. Caspase3/7 activity was measured in cells treated with 125, 250 and 500 μM I3C for 30 h. *, P<0.05 (n=6) compared to "no I3C". **B.** I3C-induced apoptosis was increased by inhibition of protein synthesis in MDA-MB-468 and HBl100 cells. Caspase3/7 activity was measured in cells treated with 10 μM of cycloheximide (CX) for 1 h, followed by 250 (MDA-MB-468) or 500 (HBL100 and MDA-MB-231) μM I3C for another 30 h. *, P<0.05 (n=6) compared to "no I3C". #, P<0.05 compared to "I3C alone".

Fig. 3. I3C-induced apoptosis was inhibited by pan-caspase inhibitor.

MDA-MB-468 cells were incubated in the presence or absence of 250 or 500 μM I3C and caspase inhibitors 10μM Z-YVAD-FMK (**A**) or 50μM Z-VAD-FMK (**B**), added 60 min prior to I3C. The percentages of live, apoptotic and necrotic cells were measured after 16 h of treatment. All data are presented as the means ±SD. *, P<0.05 versus "no I3C"; $^{\#}$, P<0.05 versus the same concentration of I3C (**A**, n=5; **B**, n=6).

Fig. 4. I3C induced apoptosis in MDA-MB-468 cells via a mitochondrial pathway.

A. The percentage of cells with normal mitochondrial membrane potential (M1) and cells that lost mitochondrial potential (M2) after treatment with 125 μM I3C for indicated number of hours (n=4). **B.** The percentage increase in caspase-8 and caspase-9 activities was measured after treatment with 125 μM I3C for the indicated number of hours (n=4). **C.** Caspase 3/7 activity was measured in cells treated with 125 and 250 μM I3C for 24 and 30 h (n=6). **D.** A percentage of live, apoptotic and necrotic cells was measured after 16-48 h of treatment with 125 μM I3C (n=6). **A-D.** All data are presented as percentage of means ±SD. *, P<0.05 versus "no I3C".

Fig. 5. Loss of mitochondrial membrane potential preceded cell death in MCF7 cells.

A. The percentage of cells with normal mitochondrial membrane potential (M1) and cells that lost mitochondrial potential (M2) after treatment with 250 μM I3C for indicated number of hours (n=3). **B.** A percentage of live, apoptotic and necrotic cells was measured during the same treatments (n=3). *, P<0.05 versus "no I3C".

Fig. 6. Human fibroblasts were resistant to I3C.

A. Caspase 3/7 activity was measured in fibroblasts treated with 250 and 500 μM I3C for 30 h (n=6). **B.** Percentages of live, apoptotic and necrotic cells was measured after 48 h of treatment with 500 μM I3C (n=8). **A-B.** The data are presented as the means ±SD. *, P<0.05 versus "no I3C". **C.** Fibroblasts grown as a monolayer and in collagen I gel were treated with I3C for 48 h. The data are presented as percentage of means ±SE. *, P<0.05 versus control cells grown in the absence of I3C. #, P<0.05 versus control cells, grown on plastic, with the same treatment (n=16).

Fig. 7. I3C downregulated EGFR expression in some breast cancer cells.

Breast cancer cells were treated with I3C for 4-12 h (A, B) and 18-30h (D). Western blots (40 μg of protein extract/lane) were developed with the antibodies indicated on the right. EGFR detection in HBL100 and MCF7 cells was performed using different ECL substrate and exposure times compared with those in other cell lines. Quantified results of 3 experiments (A and D) are shown on graphs (C and E, respectively). *, P<0.05 versus "no I3C".

Fig. 8. Viability of breast cancer cells MDA-MB-468 and MDA-MB-231 was EGFR-dependent

Caspase 3/7 activity (**A,** n=6) or viability (**B,** n=16) were measured in cells treated with 0.5-20 μM of EGFR inhibitor PD153035 for 30 h. **A-B.** The data are presented as the means ±SE. *, P<0.05 versus "no inhibitor".

Fig. 9. EGFR modulated viability of MDA-MB-468 cells in response to I3C in the 3D environment.

Viability of cells grown on plastic (**A,** n=16), in collagen I gels (**B,** n=16) or spheroids (**C,** n=8) was determined after 48 h treatment with 125 μM I3C in the presence or absence of 100 ng/ml EGF or 100 nM PD153035. **A-C.** The data are presented as the means ±SE. *, P<0.05 versus "no treatment". #, P<0.05 versus cells with the same EGFR modulation in the absence of I3C. ^, P<0.05 versus "I3C only". **D.** Two independent cultures, grown as in controls in A-C, were analyzed using western blotting (40 μg of protein extract/lane), developed with the antibodies indicated on the right. Molecular weight markers are shown on the left. **E.** Quantified results of experiment D. *, P<0.05 versus monolayer.

Fig. 1

24

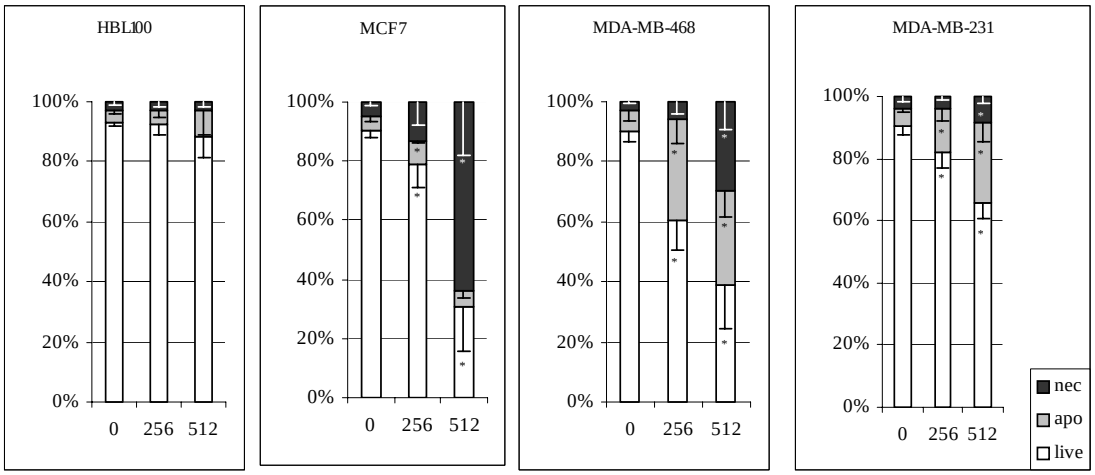
HBL100
MCF7
MDA-MB-468
MDA-MB-231
100%
80%
60%
40%
20%
0%
0
256
512
nec
apo
live

48

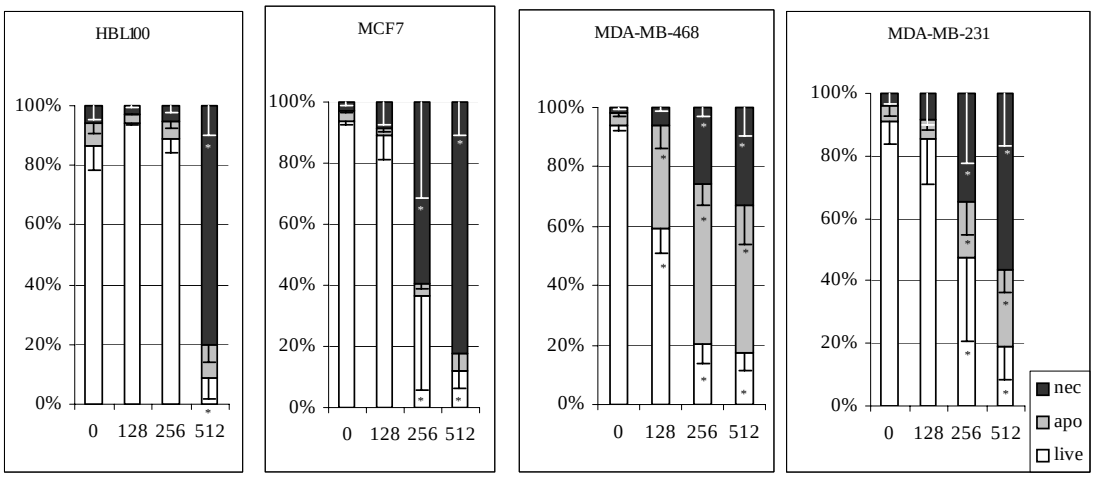
HBL100
MCF7
MDA-MB-468
MDA-MB-231
100%
80%
60%
40%
20%
0%
0
128
256
512
nec
apo
live

Fig. 2

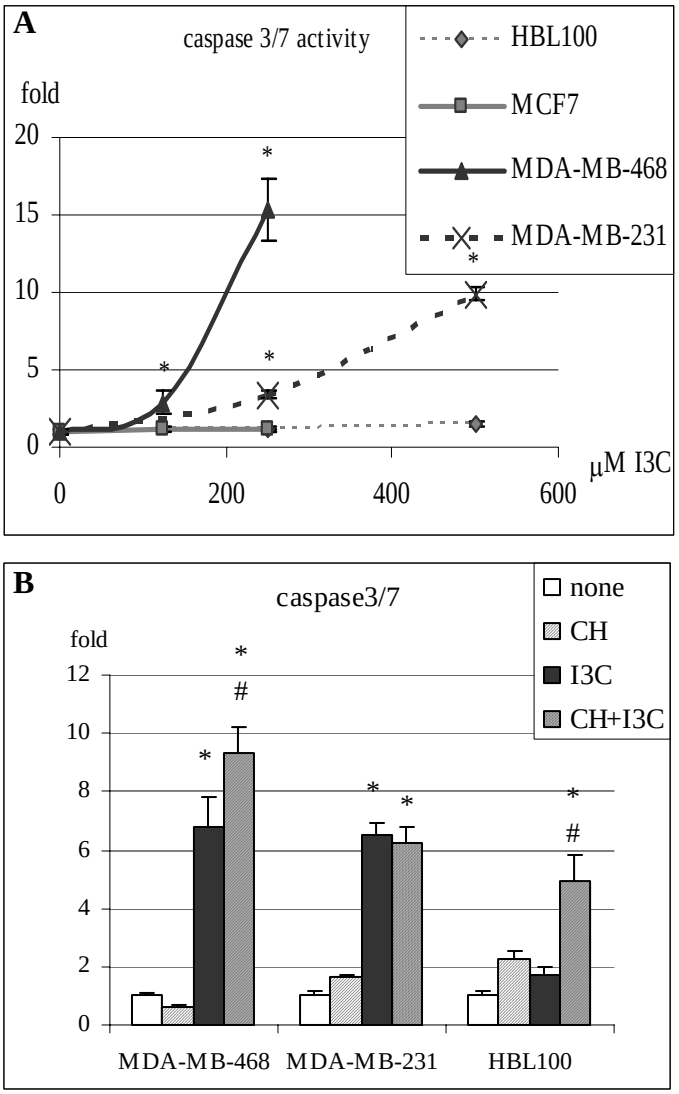
A
caspase 3/7 activity
fold
20
15
10
5
0
0
200
400
600
μM I3C
HBL100
MCF7
MDA-MB-468
MDA-MB-231
B
caspase3/7
fold
12
10
8
6
4
2
0
none
CH
I3C
CH+I3C
MDA-MB-468
MDA-MB-231
HBL100

Fig. 3

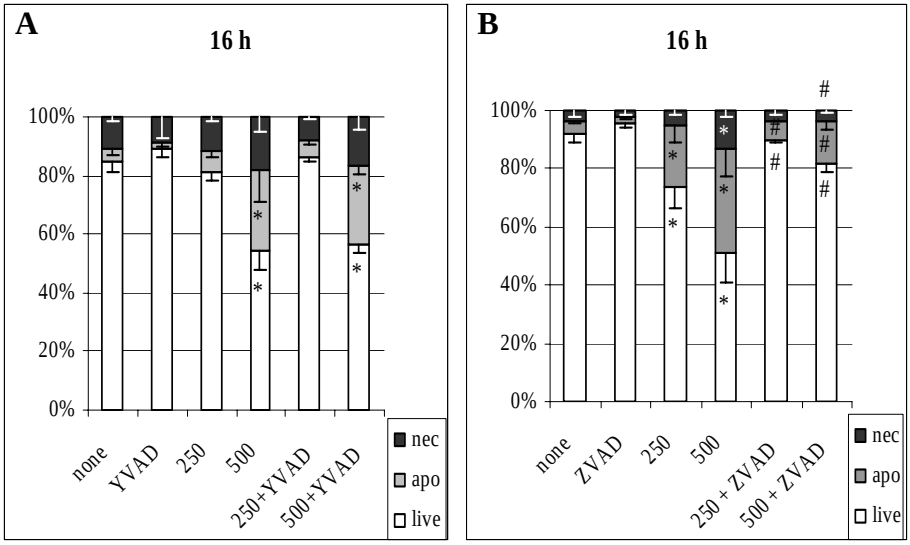
A
16 h
100%
80%
60%
40%
20%
0%
none
YVAD
250
500
250+YVAD
500+YVAD
nec
apo
live
B
16 h
100%
80%
60%
40%
20%
0%
none
ZVAD
250
500
250 + ZVAD
500 + ZVAD
nec
apo
live

Fig. 4

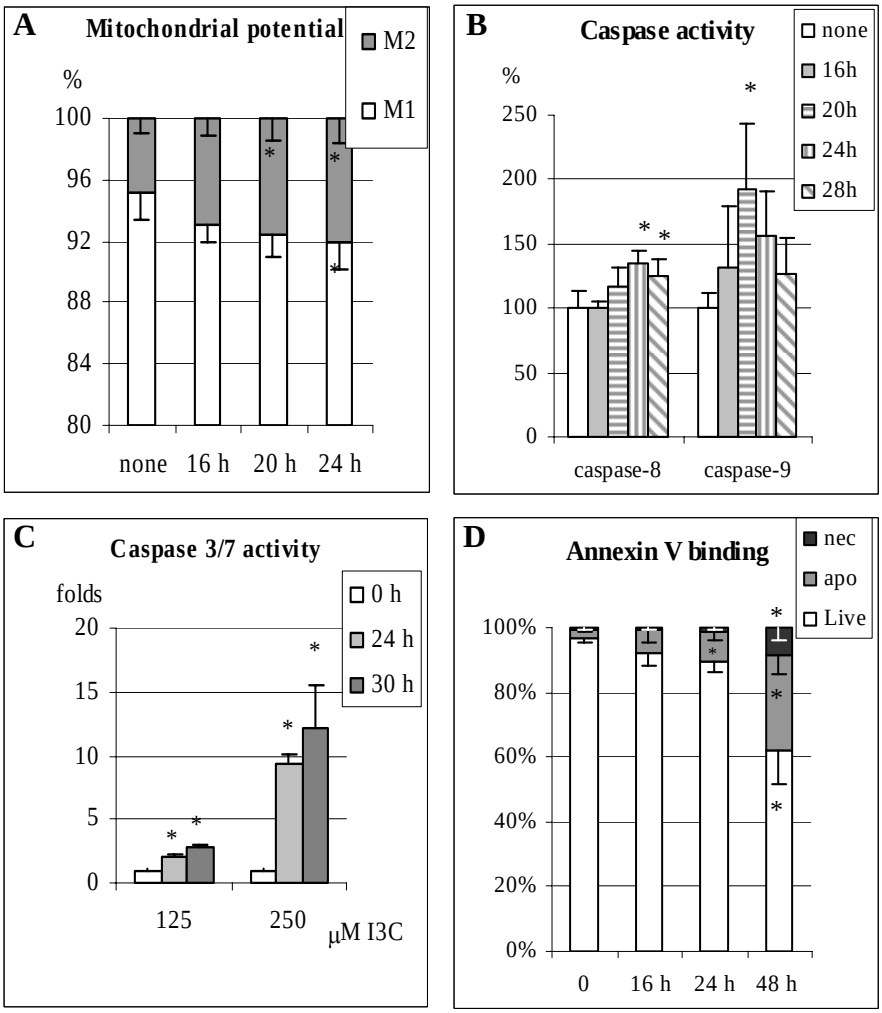
A
Mitochondrial potential
M2
M1
%
100
96
92
88
84
80
none
16 h
20 h
24 h
B
Caspase activity
none
16h
20h
24h
28h
%
250
200
150
100
50
0
caspase-8
caspase-9
C
Caspase 3/7 activity
folds
0 h
24 h
30 h
20
15
10
5
0
125
250
µM I3C
D
Annexin V binding
nec
apo
Live
100%
80%
60%
40%
20%
0%
0
16 h
24 h
48 h

Fig. 5

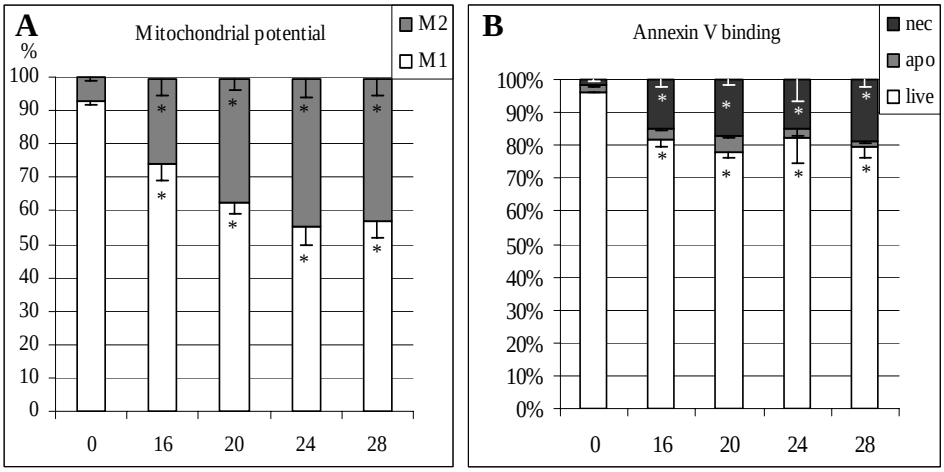
A
Mitochondrial potential
M2
M1
%
100
90
80
70
60
50
40
30
20
10
0
0
16
20
24
28
B
Annexin V binding
nec
apo
live
100%
90%
80%
70%
60%
50%
40%
30%
20%
10%
0%
0
16
20
24
28

Fig. 6

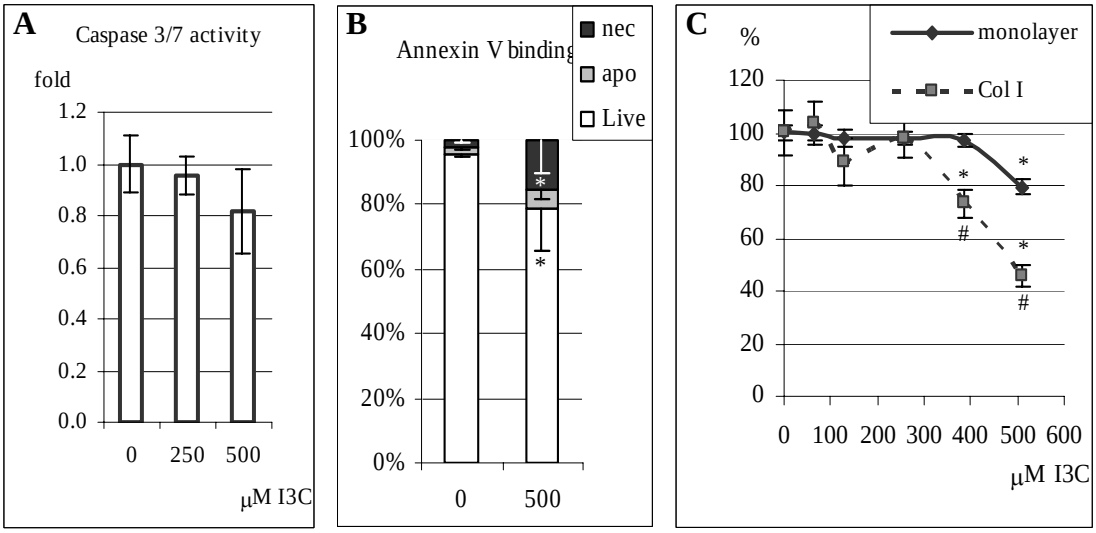
A
Caspase 3/7 activity
fold
1.2
1.0
0.8
0.6
0.4
0.2
0.0
0
250
500
μM I3C
B
Annexin V binding
nec
apo
Live
100%
80%
60%
40%
20%
0%
0
500
C
%
monolayer
Col I
120
100
80
60
40
20
0
0
100
200
300
400
500
600
μM I3C

Fig. 7

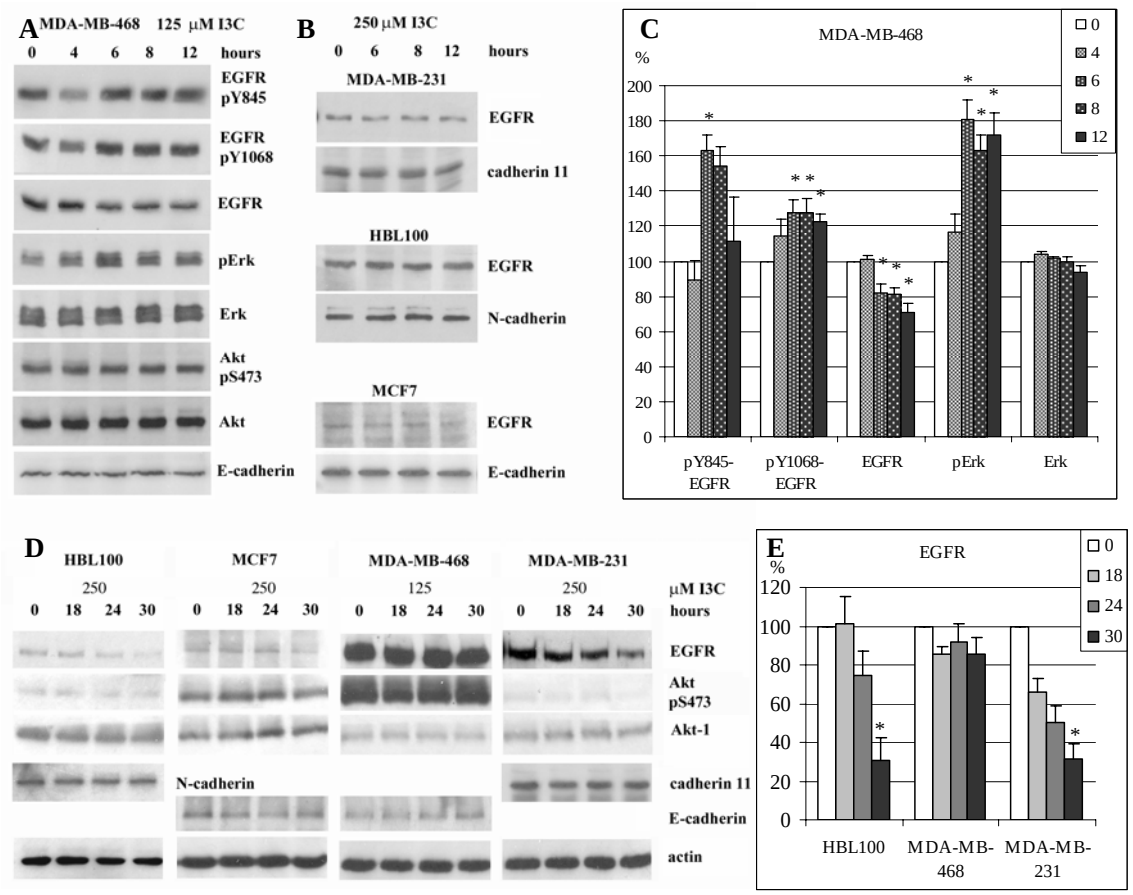
A
MDA-MB-468 125 μM I3C
0 4 6 8 12 hours
EGFR pY845
EGFR pY1068
EGFR
pErk
Erk
Akt pS473
Akt
E-cadherin
B
250 μM I3C
0 6 8 12 hours
MDA-MB-231
EGFR
cadherin 11
HBL100
EGFR
N-cadherin
MCF7
EGFR
E-cadherin
C
MDA-MB-468
%
0
4
6
8
12
pY845-EGFR
pY1068-EGFR
EGFR
pErk
Erk
D
HBL100
MCF7
MDA-MB-468
MDA-MB-231
250
125
0 18 24 30
μM I3C
hours
EGFR
Akt pS473
Akt-1
N-cadherin
cadherin 11
E-cadherin
actin
E
EGFR
%
0
18
24
30
HBL100
MDA-MB-468
MDA-MB-231

Fig. 8

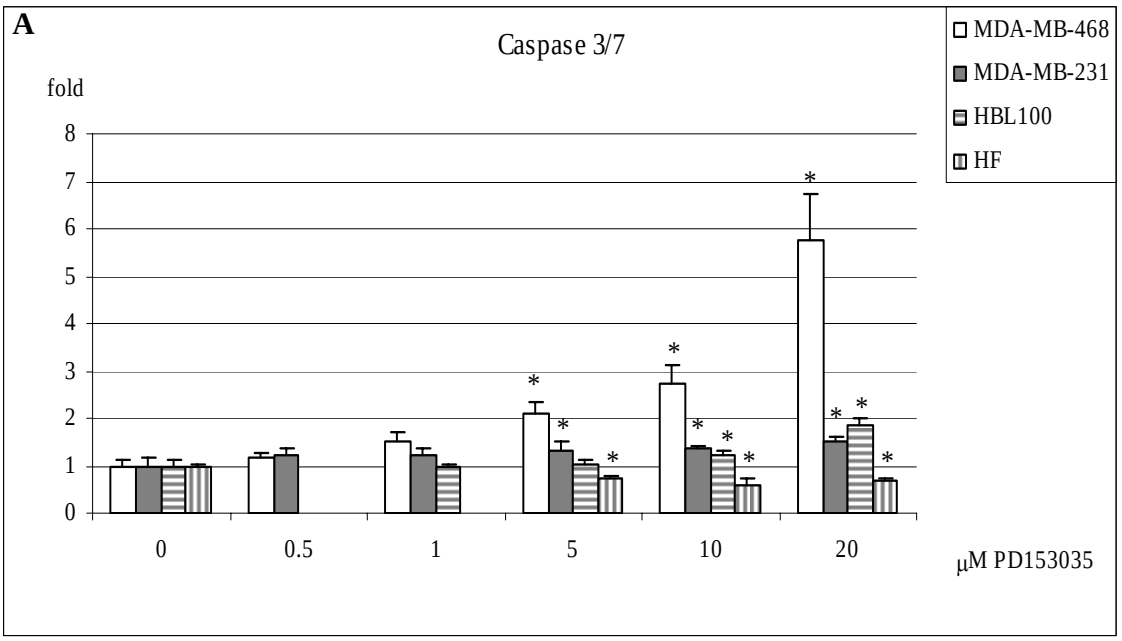
A
Caspase 3/7
fold
8
7
6
5
4
3
2
1
0
0
0.5
1
5
10
20
μM PD153035
MDA-MB-468
MDA-MB-231
HBL100
HF

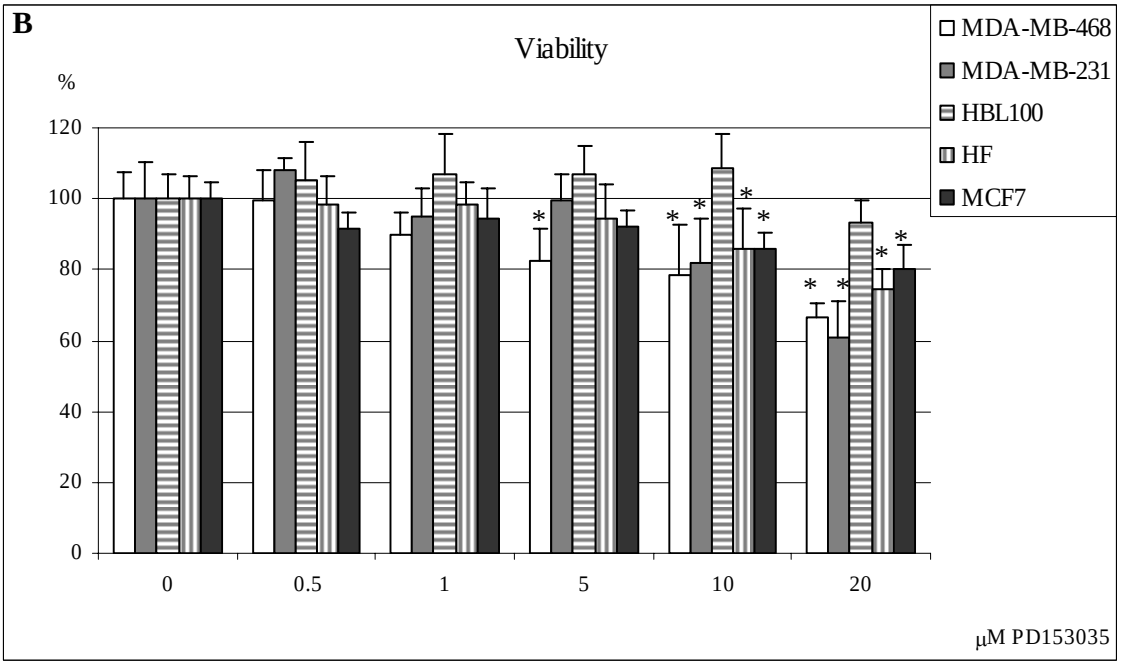
B
Viability
%
120
100
80
60
40
20
0
0
0.5
1
5
10
20
μM PD153035
MDA-MB-468
MDA-MB-231
HBL100
HF
MCF7

Fig. 9

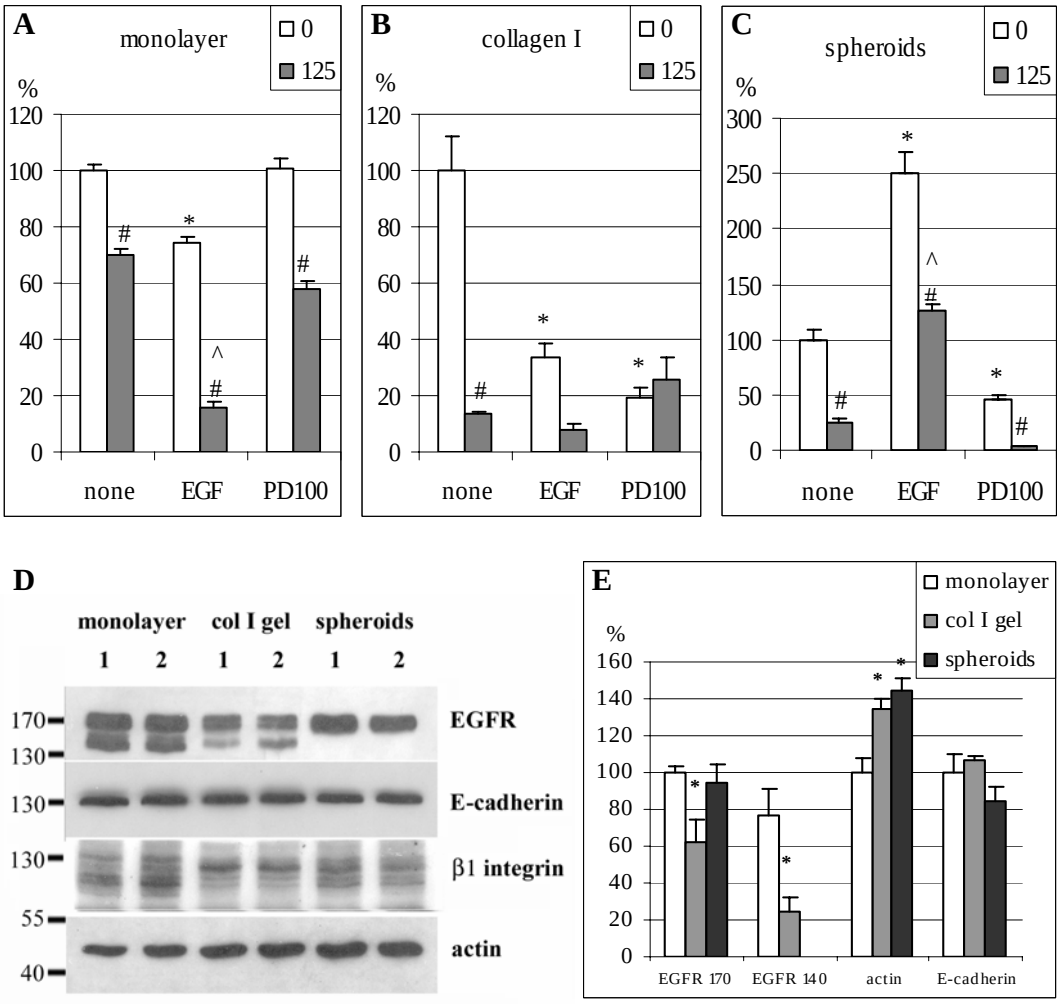
A
monolayer
0
125
%
120
100
80
60
40
20
0
none
EGF
PD100
B
collagen I
C
spheroids
300
250
200
150
100
50
D
monolayer
col I gel
spheroids
1
2
170
130
55
40
EGFR
E-cadherin
β1 integrin
actin
E
monolayer
col I gel
spheroids
160
140
EGFR 170
EGFR 140
actin
E-cadherin